Am J Transl Res 2022;14(6):4295-4309
www.ajtr.org /ISSN:1943-8141/AJTR0143899

Original Article

PKC inhibitors regulate stem cell self-renewal by regulating H3K27me3 and H3K9me3

Jialei Sun[1], Na He[2], Weiguo Wang[1], Yujian Dai[1], Chunhui Hou[3], Fuliang Du[1]

[1]Jiangsu Key Laboratory for Molecular and Medical Biotechnology, College of Life Sciences, Nanjing Normal University, Nanjing 210046, China; [2]Harbin Institute of Technology, Harbin 150001, Heilongjiang, China; [3]Shenzhen Key Laboratory of Gene Regulation and Systems Biology, Department of Biology, School of Life Sciences, Southern University of Science and Technology, Shenzhen 518055, Guangdong, China

Received May 4, 2022; Accepted June 14, 2022; Epub June 15, 2022; Published June 30, 2022

Abstract: Embryonic stem cell (ESC) research is critical to the scientific community, as their application in regenerative medicine can be widely beneficial. ESCs eventually withdraw from their self-renewal program and subsequently differentiate into specific cell lineages; however, the mechanisms regulating these processes remain unclear. PKC inhibition using 3-[1-[3-(dimethylamino) propyl]-5-methoxy-1H-indol-3-yl]-4-(1H-indol-3-yl)-1H-pyrrole-2,5-dione (PKCi) is responsible for the derivation and maintenance of human, rat, and mouse ESCs, but the mechanism by which PKCi maintains stem cell self-renewal is poorly understood. By studying the PKCi stem cell (PKCi-mESC) transcriptome and epigenetic modification, we found the transcriptome of PKCi-mESC differed from 2i stem cells (2i-mESC), with 2010 up-regulated genes and 1784 down-regulated genes. Among them, genes related to core transcription factors, naïve-specific markers, and pluripotency are differentially expressed between the two stem cell lines. We analyzed epigenetic modification of PKCi-mESC and found the distribution of H3K27me3 signal was significantly reduced at transcription start sites (TSSs) throughout the genome and at differentially expressed genes (DEGs). Likewise, the H3K9me3 signal at TSSs throughout the genome was significantly reduced in PKCi-mESC, but the distribution on DEGs is reversed. *Kdm4d* and *Kdm6a* knockdown by RNA interference (RNAi) significantly altered the expression of genes related to self-renewal in PKCi-mESC. In conclusion, we revealed PKCi-mESC and 2i-mESC differentially express numerous genes, including stem cell-related genes. Furthermore, PKCi-mESC regulated gene expression through H3K27me3 and H3K9me3 modification, which maintained stem cell self-renewal capacity.

Keywords: Mouse, mESC, PKCi, self-renewal, histone modification

Introduction

Embryonic stem cells (ESCs) [1], which are derived from the inner cell mass within the blastocyst, are pluripotent cells with the ability to differentiate into any cell type of an adult animal [2]. Not only can ESCs continuously self-renew without losing pluripotency under appropriate culture conditions, but they can also differentiate into predetermined cells when cultured with specific inducers [3, 4]. Because of this unique property, ESCs are an ideal model system for studying early mammalian development and they provide a valuable tissue source for drug screening and disease research [5]. ESCs can differentiate into all three germ layers, which holds great promise for regenerative medicine [6, 7]. To realize the full therapeutic potential of ESCs, a thorough understanding of the molecular mechanisms regulating their exit from the self-renewal program and their subsequent differentiation into specific cell lineages is required [3].

ESCs are defined by two basic characteristics: pluripotency and self-renewal [8]. Both characteristics are dependent on the coordination and balance of signal transduction pathways, transcription factor networks, and epigenetic regulators [4, 9-13]. The transition from a pluripotent state into lineage-specific differentiation is critical for mammalian development, but the molecular mechanisms that regulate lineage commitment remain poorly understood [3, 14, 15]. ESCs grown under standard conditions (i.e., medium supplemented with bovine serum

and the cytokine Leukemia Inhibitory Factor, LIF) contain a subpopulation of differentiated cells, although most cultured cells remain pluripotent and are undergoing self-renewal [15-18]. In addition, pluripotency-related transcription factor expression levels differed between ESCs grown under serum and LIF conditions. Consequently, genetically identical cells exposed to the same culture conditions exhibited functional heterogeneity [5, 13, 19, 20]. Nichols et al. maintained mouse ESC (mESC) pluripotency by adding two inhibitors to activate the JAK-STAT3 pathway or inhibit the ERK/GSK3 signaling pathway (2i) [5, 21, 22]. Dutta et al. used a small factor that inhibited protein kinase C (PKC) to maintain mESC pluripotency without activating STAT3 or inhibiting ERK/GSK3 signaling [20]. Moreover, mESC in this culture system could form chimeric mice, which can generate targeted mice. Simultaneous inhibition of PKC isoforms leads to reprogramming of mouse embryonic fibroblasts (MEF) into induced pluripotent stem cells and PKCζ plays an important role in inducing lineage development of mESCs through the NF-κB signaling pathway [20]. Taken together, this suggests regulation of mESC pluripotency is complex, and that PKC signaling is a crucial regulator of ESC self-renewal and lineage commitment. However, further research is needed to understand the mechanisms by which PKC signaling regulates ESC self-renewal.

Naïve mESCs and rat ESCs can be derived using a PKCi (3-[1-[3-(dimethylamino) propyl]-5-methoxy-1H-indol-3-yl]-4-(1H-indol-3-yl)-1H-pyrrole-2,5-dione) culture system [20, 23, 24]. Adding PKCi, 2i, LIF and other small factors to ESC cultures can also separate naïve human embryonic stem cells (hESCs) [25]. Our research group successfully isolated rabbit naïve ESCs using PKCi, 2i and LIF [26]. Furthermore, we successfully isolated mESC from C57BL/6J mice using only PKCi [24], indicating PKCi promotes or maintains the role of ESCs in different species.

Gene expression patterns are largely responsible for the differences between lineage cells and the pluripotent cells from which they originated [20, 27]. In fact, the introduction of four transcription factors can induce pluripotency in somatic cells [28, 29]. Critically, gene expression is intimately related to epigenetic modification [29-34]. Among them, H3K4me3 was enriched at the promoters of actively transcribed genes or genes with positive transcription potential [35], but H3K27me3 was associated with stable gene silencing [36]. Reduction of H3K27me3 in induced pluripotent stem cells facilitate self-renewal of ESCs and somatic cell reprogramming [3, 37, 38]. In contrast, H3K9me3 is involved in the generation of heterochromatin and also plays a significant role in lineage fidelity maintenance [39]. H3K9me3 is also a primary epigenetic determinant, and removal of this mark leads to fully reprogrammed iPSCs [40]. A bivalent site refers to a location in the genome where both activating and repressing histone marks are juxtaposed on the same nucleosome. In ESCs, bivalent genes are normally transcriptionally silent, but are rapidly activated in the appropriate lineage during embryonic development. However, the mechanisms by which epigenetic enzymes recognize these chromatin marks and interact with the core pluripotency network to regulate the balance between self-renewal and differentiation remain elusive [2]. Furthermore, there was no report of H3K9me3 and H3K27me3 epigenetic modification in PKCi derived mESC.

To better understand the mechanisms of ESC self-renewal, we profiled the transcriptomes and analyzed the epigenetic modifications of histones H3K4me3, H3K9me3, H3K27me3 and H3K27ac in mESC isolated with 2i (2i-mESC) and PKCi (PKCi-mESC).

Materials and methods

Chemicals and reagents

Unless otherwise noted, chemicals were purchased from Sigma-Aldrich (St. Louis, MO, USA).

Animals

All animal protocols were approved by the Animal Care and Use Committees of Nanjing Normal University (IACUC-20201209). This study was carried out in accordance with the recommendations of the Guide for the Care and Use of Laboratory Animals of the National Institutes of Health. Mice were maintained in a specific pathogen free animal facility at Nanjing Normal University and bred in individually venti-

lated cages (four mice per cage) with free access to food and water. The mice were kept in a 12:12 h light: dark cycle and maintained at 24±2°C and 50±20% relative humidity. All animal experiments were performed using proper anesthesia.

Embryonic stem cells

Blastocysts were seeded on Mitomycin in C-treated MEFs on 0.1% gelatin-coated plates (ES-006-B, Millipore, Burlington, MA, USA) with PKC inhibitor (5 μM Gö6983, 133053-19-7, Selleck, Houston, TX, USA) in basic culture medium supplemented with Dulbecco's Modified Eagle's Medium (DMEM; 10829018, Gibco, Gaithersburg, MD, USA) containing 15% knockout serum replacement (10828028, Gibco), 1% penicillin/streptomycin (SV30010, HyClone, Logan, UT, USA), 2 mM glutamine (35050061, Gibco), 1 mM sodium pyruvate (11360088, Gibco) and 0.1 mM 2-mercaptoethanol (ES-007-E, Millipore). Following 7 days of culture, outgrowths were collected and digested into single-cell suspensions with Accutase (A1110501, Gibco) and re-seeded in new plates coated with feeder cells. mESC were passaged by incubating colonies with Accutase. Then, mESCs were plated into a new 24-well plate coated with new feeder cells at a density of 1×10^3 cells/cm^2 at 3- to 4-day intervals. Collected mESCs were frozen in cryopreservation medium with 90% fetal bovine serum (FBS; SH30070.03, HyClone) and 10% dimethyl sulfoxide (D5879) and stored in liquid nitrogen [24].

RNA extraction and sequencing

Total RNA was isolated from the leaves of rice seedlings with the plant total RNA extraction reagent TransZol up plus RNA kit (TransGen Biotech, China). The cDNA libraries were prepared from mRNA using NE Next Ultra RNA Library Prep Kit for Illumina (NEB, USA), according to the manufacturer's instructions. The cDNA libraries were paired-end sequenced for 150 bp on both ends on an Illumina HiSeq X-Ten platform.

ChIP-seq

Sequence libraries were generated using the TruSeq Library Prep Pooling kit (Illumina 15042173), following the manufacturer's instructions. Paired-end 100-bp sequencing was performed on HiSeq 2000 (Illumina) at the Neogene [41].

qPCR

Total RNA was extracted from mESCs with Trizol reagent (T9424). Reverse transcription reactions were performed with 1 μg RNA using HiScript II Reverse Transcriptase (R223-01, Vazyme, Nanjing, China). For the qPCR reaction, cDNA was used as a template and mixed with 2xSYBR Green Fast qPCR Mix with High Rox (RM21206, ABclonal, China). Individual gene expression was normalized to *GAPDH* expression, and values from the PKCi group were defined as 1.0 for all gene expression levels. *GAPDH* was used as an endogenous control. The qPCR primers are shown in in Table S2.

Kdm4d and Kdm6a knockdown in cloned embryos

For RNAi, mouse *Kdm4d* and *Kdm6a* siRNAs were diluted in DMEM to a final concentration of 50 pM with 1 μL Entranster TM-R4000. Then, the mixture was incubated in 500 μL medium with cells for 8 h. Next, siRNAs were removed by fluid exchange and culture continued for 24 h. The siRNAs are shown in in Table S3.

Statistical analyses

On-target and off-target mutation frequencies were analyzed using SPSS software (SPSS 18.0, IBM). The percentage data in each replicate were arcsine transformed and subjected to one-way ANOVA. Means were compared by Fisher's least significant difference test (PLAS). The threshold for statistical significance was $P < 0.05$. Significant difference was indicated by *, **among the groups (*, $P < 0.05$; **, $P < 0.01$).

Analysis of RNA-seq

Sequencing data were mapped to mouse genome (mm9) normal chromosome and X chromosome by STAR with default parameter. Then only kept the uniquely mapped reads with samtools parameter "-q 30", and removed the duplicate reads with Picard tools with default parameter. Remain reads were count by HTseq-count with default parameter. Count matrix

were used as input to calculate gene FPKM and differentially expressed genes by DEseq2. DEGs were genes with p value < 0.01 and fold change larger than 3. R package pheatmap was used to plot the heatmap of z score of FPKM in each gene.

Analysis of ChIP-seq

Sequencing data were mapped to mouse genome (mm9) normal chromosome and X chromosome by bowtie2 with parameter "-N 1 -L 25 -X 2000 -5 7 -3 80 --no-mixed --no-discordant". Then only kept the uniquely mapped reads with samtools parameter "-q 20", and removed the duplicate reads with Picard tools with default parameter. RPKM of histone modification ChIP data were calculated by deeptools bamCoverage command with parameter "-bs 200". Peaks were called by macs2 with parameter "-g mm" for H3K27ac and H3K4me3 each replicate, with parameter "--broad -g mm" for H3K9me3 and H3K27me3 each replicate. Final peaks were the merge of overlapped peaks between each replicate.

Distribution of histone modification in genome were implemented by R package ChIPseeker that peaks of each histone modification were imported and TSS +/- 1000 bp was assigned as promoter region.

To obtain the histone modification enrichment signal around genes, RPKM matrix of histone modification were used to calculated the signal around gene +/- 5 kb region with bin size 200 by deeptools computeMatrix command. Then we plotted the signal with plot Heatmap command.

Data availability

ChIP-seq and RNA-seq datasets have been deposited in the Sequence Read Archive (SRA) under the accession number PRJNA849820, and are accessible for reviewers: at https://www.ncbi.nlm.nih.gov/sra/PRJNA849820.

Discussion

The successful derivation and culture of ESCs has great implications for medicine. However, the intrinsic molecular mechanisms regulating ESC biology remain largely unknown. We revealed that 2i-mESC and PKCi-mESC have different transcriptional profiles, despite being naïve state stem cells. Not only do these results indicate that mESCs are heterogeneous, but they suggest mESCs can be regulated by gene expression related to self-renewal. Using ChIP-seq, we identified differences in epigenetic modification between PKCi-mESC and 2i-mESC. Among them, H3K9me3 distribution was similar throughout the whole genome, but there were stark differences in H3K4me3, H3K27me3 and H3K27ac distribution. The signal of H3K27me3 in PKCi-mESC had a proportion of the promoter region of 32.9%, less than the 37.0% observed in 2i-mESC. The H3K27me3 distal intergenic region in PKCi-mESC accounts for 19.0% compared to the 25.9% in 2i-mESC. Lastly, the PKCi-mESC have the H3K27me3 proportion of 37.0% in the gene body, which was more than 27.9% in 2i-mESC. The gene-wide distribution of histone modifications of H3K27ac corroborates these results. We speculate PKCi-mESC maintenance is related to H3K27me3 distribution. Examination of the H3K4me3 whole gene distribution map revealed the ratio of PKCi-mESC in the promoter is larger than 2i-mESC, but the H3K4me3 ratio in the distal intergenic is less than 2i-mESC. Taken together, these findings suggest the ability of PKCi-mESC to maintain the self-renewal may be related to regulation of H3K27me3 and H3K4me3 modification, which may control expression of self-renewal genes.

PKC inhibitors [20] have been used to successfully isolate and maintain embryonic stem cells by promoting self-renewal, which has provided more opportunities to study mESCs [24] and hESCs [25]. Through the analysis of the transcriptome and epigenetic modification of mESCs cultured with PKCi, we found the level of H3K27me3 modifications in PKCi-mESC was significantly decreased in the promoter segment, increased in the distal intergenic interval, and these modifications were specific for mESC. We used RNAi to knockdown *Kdm4d*, a demethylase of H3K9me3, and *Kdm6a*, a demethylase of H3K27me3, in PKCi-mESC and determined these methylases significantly regulate the expression profiles of stem cell-related genes.

Our results show PKCi regulates H3K27me3 modification by increasing methylase expression, such as *Kdm6a*, reducing the inhibition of genes that are necessary for mESC maintenance. Simultaneously, PKCi regulates H3K9-

me3 modification to inhibit the high expression of differentiation-specific genes. This may be a novel mechanism for regulating gene expression in ESCs.

Furthermore, we found the NuRD-related components in PKCi-mESC were affected. For example, MBD3 decreased significantly, but the HDAC components were largely unaffected (data not shown). However, HDAC can bind to the PWWP domain to form an activation region leading to H3K27ac modification [47] and genes associated with the PWWP domain were highly expressed in PKCi-mESC (data not shown). At the same time, HDAC competes with MBD3 for the MTA1 binding site, which explain the small MBD3 decrease and HDAC reduction. The NuRD complex is known to regulate cellular transcriptional profiles by restricting lineage-specific enhancers and promoters [48]. These sites are identified by NuRD components, such as HDAC1/2 and MAT1 [49]. However, H3K27me3 modifications in enhancer and promoter regions was significantly reduced in PKCi-mESC. In total, this suggests PKCi may regulate promoter and enhancer levels of H3K27ac and H3K27me3 through the NuRD complex thereby regulating the expression of genes required for stem cells and self-renewal maintenance. However, the mechanisms by which PKC inhibitors regulate histone demethylases and histone modifications still needs to be further explored.

We found that although mESC under different PKCi and 2i condition were naïve stem cells [24], their transcriptional profiles were different. In addition to demonstrating the heterogeneity of mESCs, it is possible to identify genes with both high expression and low expression in various mESC, and further understand the mechanism of maintaining pluripotency of naïve mESC.

Results

PKCi-mESC and 2i-mESC have different transcriptional profiles

We applied DESeq to analyze differentially expressed genes (DEGs). DEGs between different samples were identified based on a Fold Change ≥ 3 and *P*-value < 0.05 [41]. Our analysis identified 3794 DEGs between PKCi-mESC and 2i-mESC. Specifically, 2010 genes were up-regulated and 1784 genes were down-regulated (**Figure 1A**, see NCBI's SPA module). However, these are both naïve mESCs, which indicates the genes that maintain mESC stemness have a certain elastic range and verifies the heterogeneity of ESCs.

An analysis of pluripotency genes, naïve genes and primed genes revealed PKCi-mESC and 2i-mESC have different gene expression characteristics (**Figure 1B-E**). Examination of core transcription factor markers [3] revealed *Pou5f1* was highly expressed in PKCi-mESC, whereas *Sox2* and *Nanog* were highly expressed in 2i-mESC (**Figure 1B**). Regarding naïve-specific markers [3], *Klf17*, *Dnmt3l* and *Rex1* were highly expressed in PKCi-mESC, whereas *Fgf4, Klf4*, *Tbx3* and *Dppa5a* were highly expressed in 2i-mESC (**Figure 1C**). Pluripotency genes [3, 42], such as *c-Myc* and *Lin28a*, were highly expressed in PKCi-mESC (**Figure 1D**). Concerning, primed-specific markers [3], *Zic2, Sfrp2*, *Otx2* and *Fgf5* were highly expressed in PKCi-mESC, whereas *Stc1* and *Hmx2* were highly expressed in 2i-mESC (**Figure 1E**). Next, we performed KEGG clustering analysis on the differential genes between PKCi-mESC and 2i-mESC. We found DEGs were enriched in Wnt, MAPK and PI3K-AKT signaling pathways, which were lowly expressed in PKCi-mESC (**Figure 1F**; Table S1). Additionally, we found DEGs were enriched in chemokine, focal adhesion and ECM-receptor interaction signaling pathway, which were highly expressed in PKCi-mESC (**Figure 1F**; Table S1). These results indicate that self-renewal regulation by PKCi may be related to the inhibition of Wnt pathway, cell-to-cell communication and extracellular matrix interaction. Furthermore, the differences in enriched pathways suggest it may be possible to obtain extracellular stem cell factors.

Because PKCi-mESC were transcriptionally distinct from 2i-mESC, we decided to examine their epigenetic modifications, as gene expression is affected by epigenetic modifications.

PKCi-mESC histone modification was biased

We analyzed several common histone modifications between PKCi-mESC and 2i-mESC, which revealed PKCi-mESC histone modification was biased compared to 2i-mESC. In PKCi-mESC, H3K27me3 accounted for 32.9% of the pro-

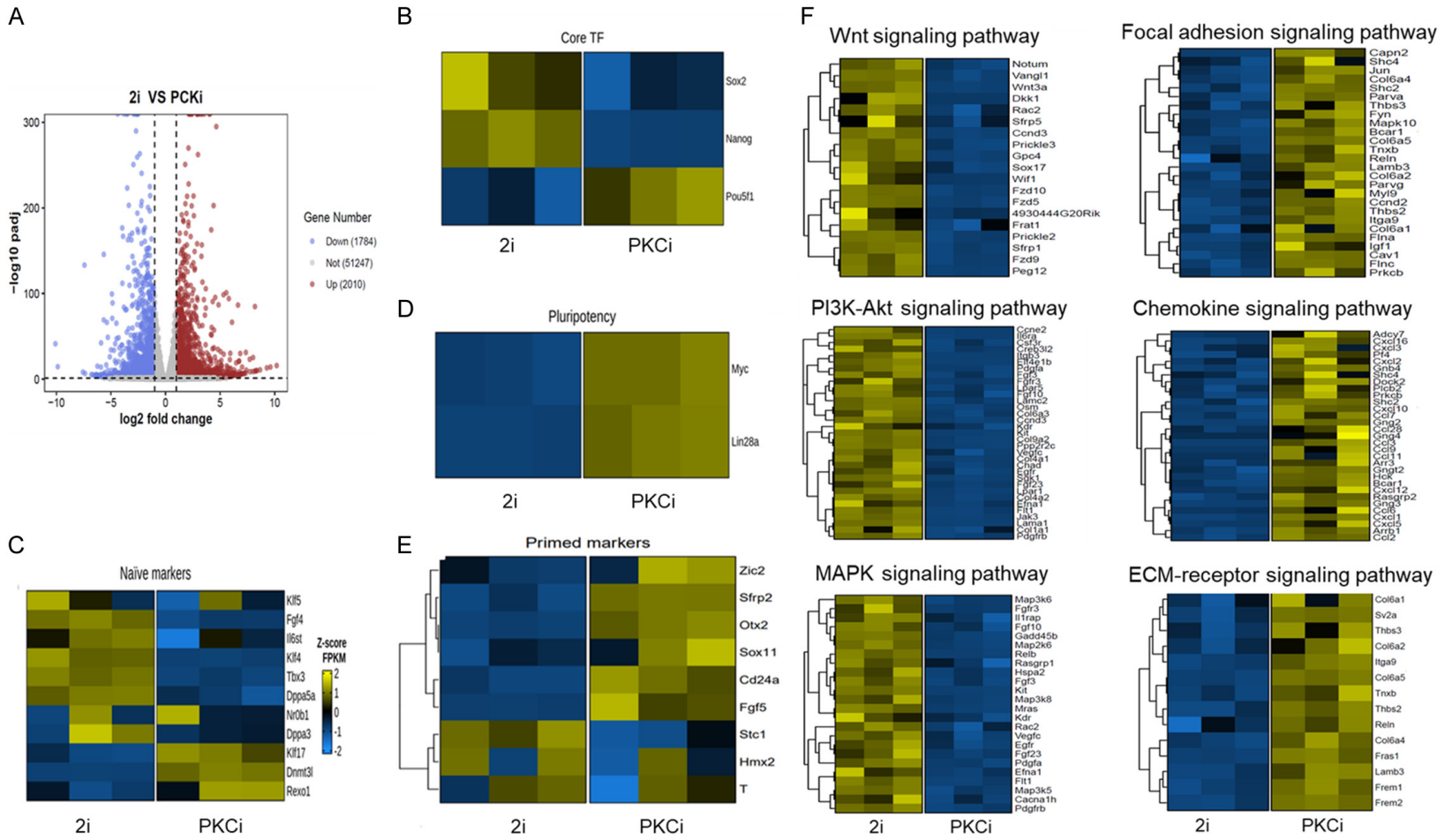

Figure 1. Transcriptomes of PKCi-mESC and 2i-mESC are significantly different. A. Volcano plot of differentially expressed genes (DEGs) between PKCi-mESC and 2i-mESC. B. Heatmap comparing transcription levels of core transcription factors in PKCi-mESC and 2i-mESC. The expression level of *Pou5f1* was significantly (FC > 2) increased in PKCi-mESC, but *Sox2* and *Nanog* expression were higher in 2i-mESC. C. Heatmap comparing transcription levels of naïve-specific markers in PKCi-mESC and 2i-mESC. *Klf17*, *Dnmt3l* and *Rex1* genes were highly expressed in PKCi-mESC, whereas *Fgf4*, *Klf4*, *Tbx3* and *Dppa5a* genes are highly expressed in 2i-mESC. D. Heatmap comparing transcription levels of pluripotency gene in PKCi and 2i. c-*Myc* and *Lin28a* were highly expressed in PKCi. E. Heatmap comparing transcription levels of primed-specific markers gene in PKCi-mESC and 2i-mESC. *Zic2*, *Sfrp2, Otx2,* and *Fgf5* were highly expressed in PKCi-mESC, whereas *Stc1* and *Hmx2* were highly expressed in 2i-mESC. F. Heatmap comparing transcription levels of DEGs between PKCi-mESC and 2i-mESC which were enriched by KEGG clustering analysis. The DEGs were enriched in Wnt, MAPK and PI3K-AKT signaling pathways, and were lowly expressed in PKCi-mESC. The DEGs were enriched in Chemokine, Focal adhesion, and ECM-recenter interaction signaling pathway, and were highly expressed in PKCi-mESC. PKCi: PKCi-mESC, 2i: 2i-mESC.

moter region, 37.0% of the gene body and 19.00% of the distal intergenic region. In 2i-mESC, H3K27me3 accounted for 37.0% of the promoter region, 27.90% of the gene body and 25.9% of the distal intergenic region. H3K4me3 accounted for 59.2% of the promoter region and 19.9% of the distal intergenic region in PKCi-mESC. In contrast, H3K4me3 accounted for 49.7% of the promoter region and 25.1% of the distal intergenic region in 2i-mESC. The proportion of H3K4me3 in PKCi-mESC was 5.2% smaller than that in 2i-mESC, which was 7.4% and the difference was mainly concentrated in the first intron segment. The H3K27ac distribution was the opposite of the H3K27me3 distribution (**Figure 2A**). In PKCi-mESC, H3K4me3 and H3K27ac were preferentially located in the promoter region (**Figure 2B**, **2D**), had a reduction of H3K27me3 modification (**Figure 2C**), and had elevated H3K27ac rather than H3K4me3 in the distal intergenic region compared to 2i-mESC (**Figure 2A**). The PKCi-mESC distribution of H3K9me3 in the TSS was significantly higher than 2i-mESC (**Figure 2E**). In addition, the H3K27me3 signal in the 5'UTR region in the PKCi-mESC was significantly higher than that in the 2i-mESC (**Figure 2A**). In summary, PKCi-mESC regulate genes expression through epigenetic modification, including decreased H3K27me3 modification in the promoter region and the distal intergenic region, elevated H3K9me3 and increased H3K27me3 modifications in the gene body and 5'UTR. We speculate that regulation of gene expression by PKCi is closely related to H3K27me3 and H3K9me3 modification.

H3K27me3 modification signal of stem cell-specific genes (green triangle markers gene) in PKCi-mESC were greatly reduced in the proximal TSS segment. In addition, H3K9me3 in the TTS segment were significantly reduced in PKCi-mESC (Figure S1).

PKCi regulated genes are associated with H3k27me3 and H3k9me3 modifications

We analyzed histone modifications around DEGs between PKCi-mESC and 2i-mESC. The H3K27ac modification in the TSS segment was significantly higher in the high expression of PKCi than that in the 2i (**Figure 3A**, **3C**), but the signal was similar in the low expression group (**Figure 3B**, **3D**). However, we found the H3K27me3 signal in the TSS segment was significantly lower in PKCi-mESC compared to 2i-mESC, whereas the H3K4me3 signal was similar (**Figure 3C**, **3D**). Furthermore, the H3-K9me3 signal in PKCi-mESC before TSSs was significantly lower than that in 2i-mESC in the high expression group (**Figure 3A**, **3C**), but this signal was higher than 2i-mESC in the low expression group (**Figure 3B**, **3D**). Based on these results, PKCi may regulate gene expression by regulating the modification of H3K27-me3, H3K27ac and H3K9me3 in the proximal region of the TSS. We speculate that PKCi maintains the expression of self-renewal genes required by reducing H3K27me3 modifications at the proximal promoter and controls gene expression by increasing H3K9me3 and H3K27me3 modifications on the gene body.

Distribution of histone modifications on stem cell-specific genes

We defined stem cell-specific genes as genes that are not differentially expressed between PKCi-mESC and 2i-mESC and are not transcribed in MEFs and cumulus cells.

A total of 51,607 genes were not differentially expressed between PKCi-mESC and 2i-mESC. To further identify stem cell-specific genes, we included genes with expression levels in PKCi-mESC and 2i-mESC three times or higher than that of MEF and cumulus when MEF and cumulus FPKM values were greater than 10. Additionally, we included genes from PKCi-mESC and 2i-mESC with FPKM values greater than 50 when the corresponding MEF and cumulus FPKM values were less than 10. This process identified a total of 162 genes candidate stem cell-specific genes. We analyzed histone modifications of these 162 genes compared to that of the whole genome.

Compared with 2i-mESC, the H3K27me3 modification signal of stem cell-specific genes in PKCi-mESC were greatly reduced in the proximal TSS segment, whereas H3K4me3 and H327ac signals were enhanced (**Figure 4A**, **4B**). In addition, the H3K27me3 signal intensity in the distal intergenic region and H3K9me3 signal intensity in the TTS (Transcription termination sites, TTS) segment were significantly enhanced (**Figure 4A**, **4C**, **4D**). These findings further suggest PKCi regulates self-renewal by reducing H3K27me3 modification target genes and increasing H3K4me3, H3K27ac and

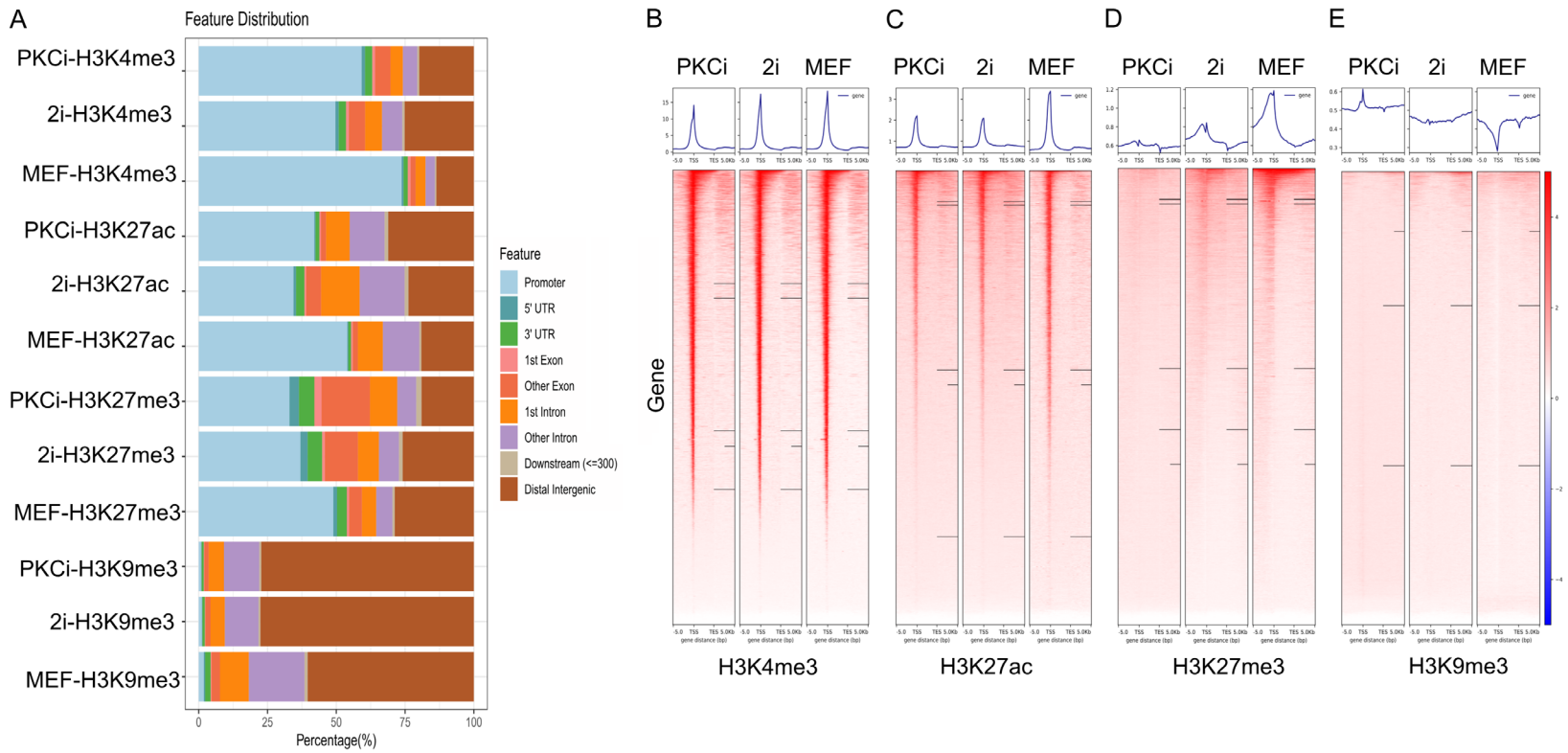

Figure 2. Genome-wide distribution of the peaks of ChIP-seq in PKCi-mESC, 2i-mESC and MEF. A. The genome-wide distribution of H3K4me3, H3K27ac, H3K27me3 and H3K9me3 peaks. The PKCi-mESC peaks reveal different histone modifications. The ChIP-seq signal in MEF represents a negative control. B. Heatmap of the distribution of H3K4me3 peaks in three types of cells. C. Heatmap of the distribution of H3K27me3 peaks in three types of cells. D. Heatmap of the distribution of H3K27ac peaks in three types of cells. E. Heatmap of the distribution of H3K9me3 peaks in three types of cells. The average ChIP-seq intensity of the four histone modifications in three cell types are shown within TSS and TTS, compared with 5 kb flanking regions. Reads counts are normalized by input, total mapped reads and region length. PKCi: PKCi-mESC, 2i: 2i-mESC.

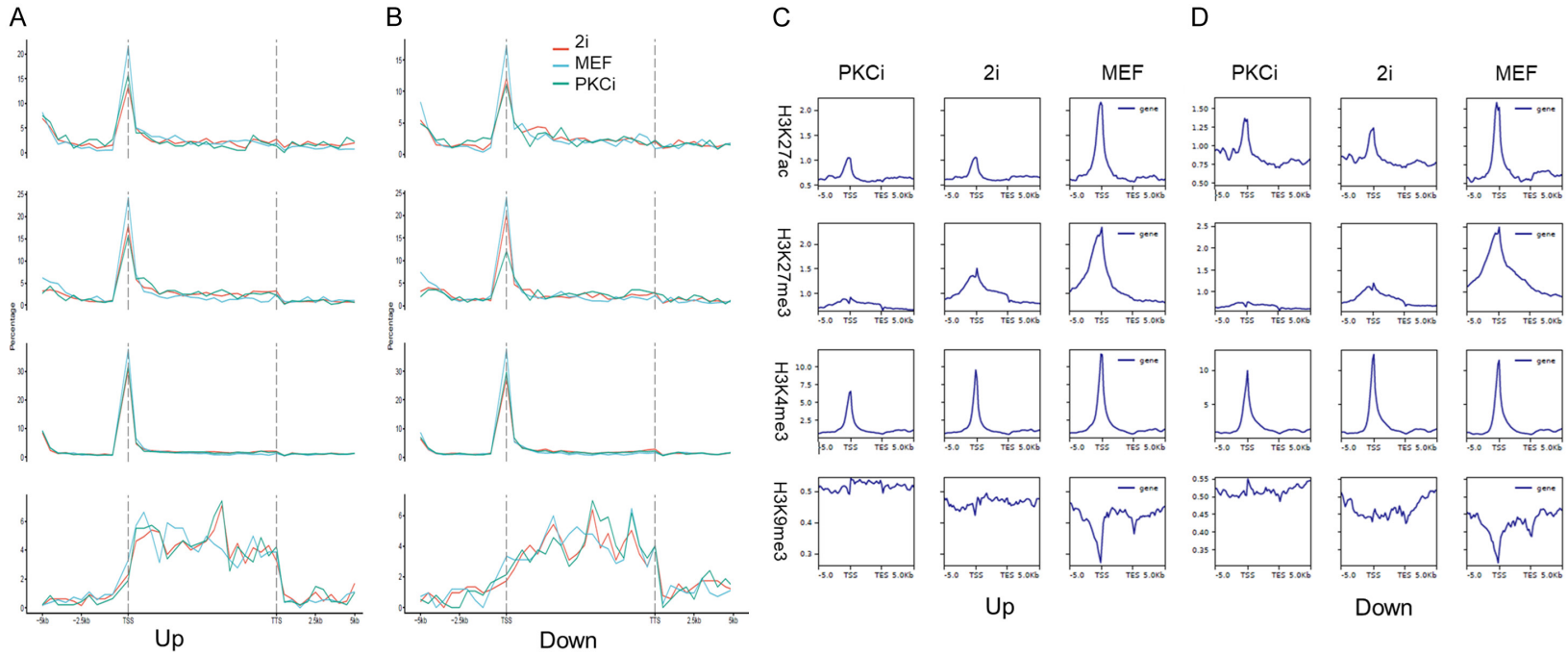

Figure 3. The distribution of DEGs from PKCi-mESC and 2i-mESC of the peaks of ChIP-seq in PKCi-mESC, 2i-mESC and MEFs. A. The peaks of ChIP-seq distributed in DEGs, which were highly expression in PKCi-mESC with H3K4me3, H3K27ac, H3K27me3 and H3K9me3. The TSS segment of PKCi-mESC highly expressed genes had decreased H3K27me3 and H3K9me3 modifications and increased H3K27ac. B. The peaks of ChIP-seq distributed in DEGs which were lowly expression in PKCi-mESC with H3K4me3, H3K27ac, H3K27me3 and H3K9me3. The TSS segment of PKCi-mESC lowly expressed genes had decreased levels of H3K27me3, but increased H3K9me3. The signal of the ChIP-seq in MEF represents the negative control. C. Heatmap of the histone profile of the highly expressed genes in PKCi-mESC compared to 2i-mESC. D. Heatmap of the histone profile of the lowly expressed genes in PKCi-mESC compared to 2i-mESC. The signal of the ChIP-seq in MEF is a negative control. PKCi: PKCi-mESC, 2i: 2i-mESC.

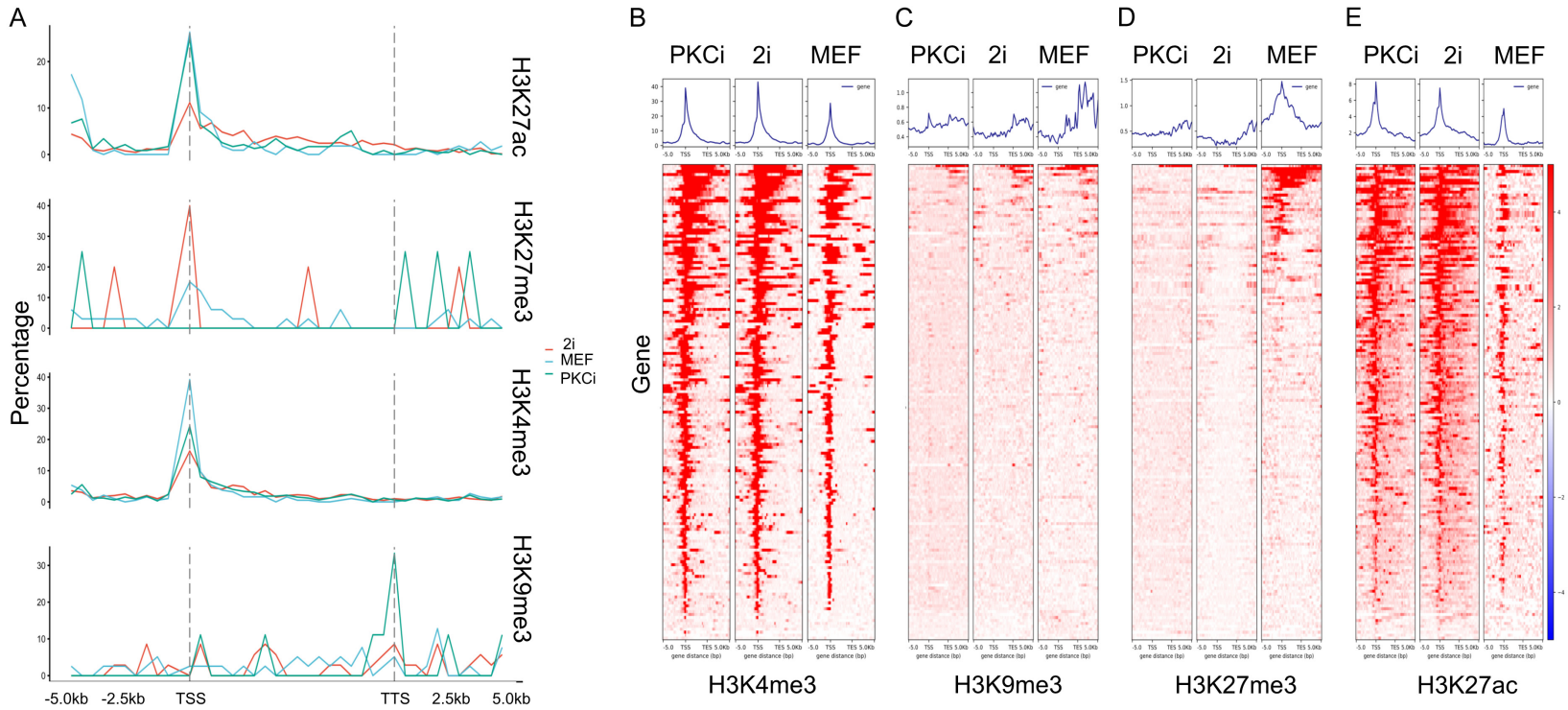

Figure 4. The enrichment bins of histone modification in the common genes between PKCi-mESC and 2i-mESC, but not expressed in MEFs and cumulus cells. A. The H3K27me3 modification signal of stem cell-specific genes in PKCi-mESC were greatly reduced in the proximal TSS segment, whereas the H3K4me3 and H327ac signals were enhanced. In addition, H3K27me3 signal intensity in the distal intergenic region and H3K9me3 in the TTS segment were significantly enhanced. B. The histone H3K4me3 profile of the common genes between PKCi-mESC and 2i-mESC, but not expressed in MEFs and cumulus cells. C. The histone H3K9me3 profile of the common genes between PKCi-mESC and 2i-mESC, but not expressed in MEFs and cumulus cells. D. The histone H3K27me3 profile of the common genes between PKCi-mESC and 2i-mESC, but not expressed in MEFs and cumulus cells. E. The histone H3K27ac profile of the common genes between PKCi-mESC and 2i-mESC, but not expressed in MEFs and cumulus cells. PKCi: PKCi-mESC, 2i: 2i-mESC.

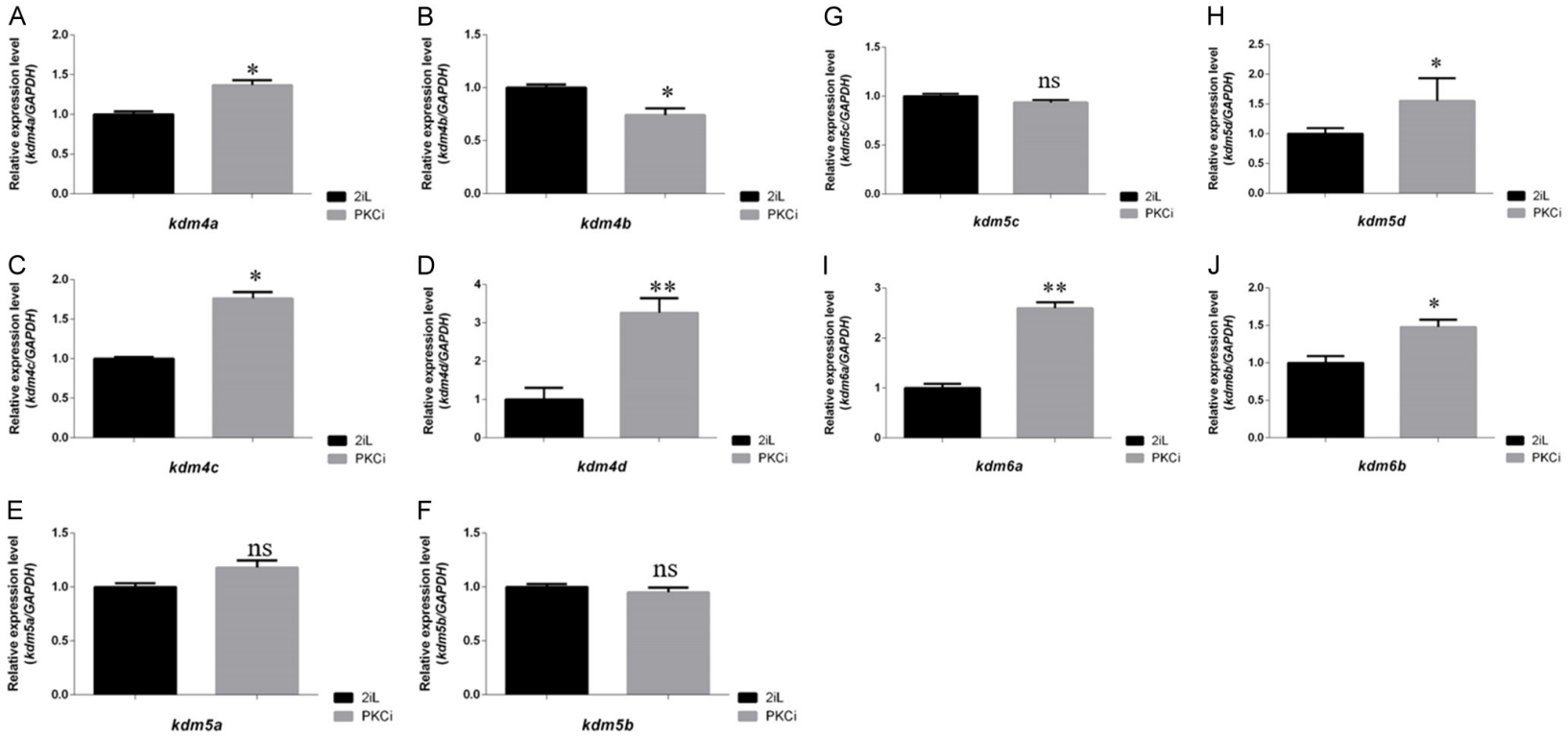

Figure 5. Bar graph showing the expression of histone demethylase in stem cells. *Kdm4a* (A), *Kdm4c* (C), *Kdm4d* (D), *Kdm5d* (H) and *Kdm6a* (I) expression was significantly higher in PKCi-mESC compared to 2i-mESC. *Kdm5a* (E) and *Kdm6b* (J) expression was higher in PKCi-mESC compared to 2i-mESC. *Kdm5c* (G) and *Kdm5b* (F) expression was similar in the two groups of stem cells. *Kdm4b* (B) expression was lower in PKCi-mESC compared to 2i-mESC. * $P < 0.05$, ** $P < 0.01$. ns, not significant. PKCi: PKCi-mESC, 2i: 2i-mESC.

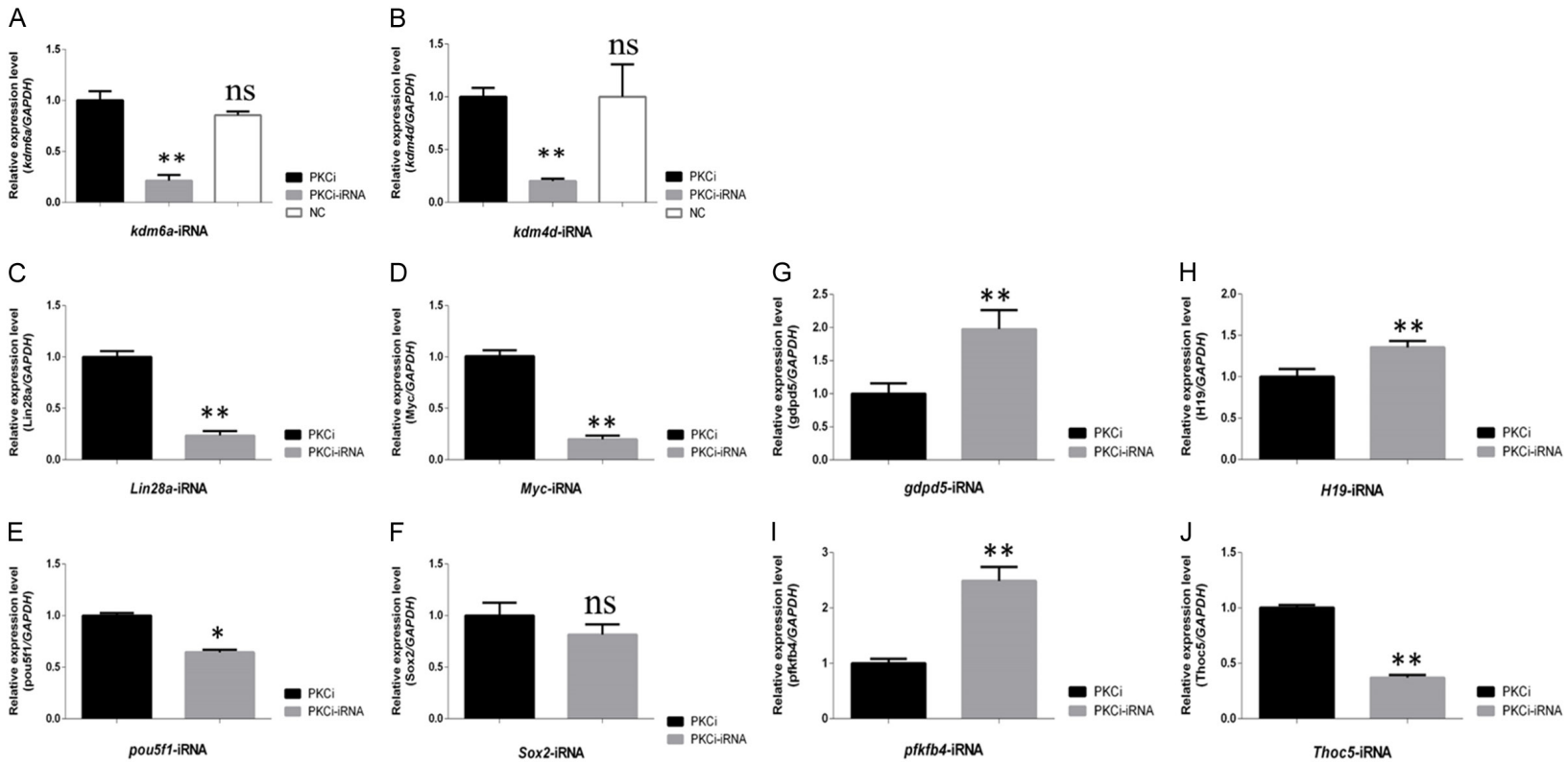

Figure 6. Knockdown of *Kdm4d* and *Kdm6a* reduces expression of stem cell-related genes. A, B. *Kdm4d* and *Kdm6a* gene expression in PKCi-mESC was knocked down by RNAi and PKCi is the expression level of the gene in PKCi-mESC, PKCi-iRNA is the expression of the gene in the cell of knocked down by RNAi. NC is a random ncRNA corresponding to RNAi. C-E. *Lin28a*, *Myc* and *Pou5f1* expression levels were significantly decreased in knockdown cell lines. F. *Sox2* expression was down-regulated, but the down-regulation was not obvious. G-I. Differentiation-related gene (*Gdpd5*, *H19* and *Pfkfb4*) expression was up-regulated in knockdown cell lines. J. In RNAi knockdown stem cells, *Thoc5* expression was significantly reduced. * $P < 0.05$, ** $P < 0.01$. ns, not significant. PKCi: PKCi-mESC, 2i: 2i-mESC.

H3K9me3 modifications to maintain expression of stem cell-specific genes.

Kdm4d and Kdm6a extremely affect PKCi-mESC self-renewal

H3K27me3 and H3K9me3 have obvious changes in PKCi-mESC compared to 2i-mESC. Therefore, we explored expression of demethylases in these two stem cell populations. We found that expression of Kdm4a (5A), Kdm4c (5C), Kdm5d (5H) and Kdm6b (5J) were significantly higher in PKCi-mESC compared to 2i-mESC. while Kdm4d and Kdm6a was extremely higher ($P < 0.01$, **Figure 5D**, **5I**). Kdm5a (5E) expression was higher in PKCi-mESC compared to 2i-mESC. Kdm5c (5G) and Kdm5b (5F) expression was similar in the two groups of stem cells. Kdm4b (5B) expression was lower in PKCi-mESC compared to 2i-mESC (Table S2). Subsequent *Kdm4d* and *Kdm6a* knockdown by RNAi (**Figure 6A**, **6B**; Table S3) in PKCi-mESC significantly reduced the expression of naïve-related genes (*Lin28a*, *Myc* and *Pou5f1*) (**Figure 6C-E**). In addition, differentiation-related genes (*Gdpd5*, *H19* and *Pfkfb4*) [43, 44] were significantly overexpressed (**Figure 6G-I**). *Thoc5* [45, 46] is an essential growth factor for stem cells maintenance, cytokine-mediated differentiation and proliferation. In RNAi knockdown stem cells, *Thoc5* expression was significantly reduced (**Figure 6J**), suggesting *Kdm4d* and *Kdm6a* may promote PKCi-mESC self-renewal.

Acknowledgements

This study was supported in part by the Natural Science Foundation of China (NSFC) (Grant No. 31872353, 32072732, 31340041 and 31471388) and Priority Academic Program Development of Jiangsu Higher Education Institutions to FD and the National Key R&D Program of China (2018YFC1004500), The Stable Support Plan Program of Shenzhen Natural Science Fund (20200925153547003), Shenzhen Innovation Committee of Science and Technology (ZDSYS20200811144002008), and Southern University of Science and Technology (No. G02226301 and Y01501821) to CH.

Disclosure of conflict of interest

None.

Address correspondence to: Dr. Fuliang Du, Jiangsu Key Laboratory for Molecular and Medical Biotechnology, College of Life Sciences, Nanjing Normal University, #1 Wenyuan Rd, Nanjing 210046, China. E-mail: fuliangd@njnu.edu.cn; Dr. Chunhui Hou, Shenzhen Key Laboratory of Gene Regulation and Systems Biology, Department of Biology, School of Life Sciences, Southern University of Science and Technology, Shenzhen 518055, Guangdong 518055, China. E-mail: houch@sustech.edu.cn

References

[1] Evans MJ and Kaufman MH. Establishment in culture of pluripotential cells from mouse embryos. Nature 1981; 292: 154-156.

[2] Takahashi S, Kobayashi S and Hiratani I. Epigenetic differences between naive and primed pluripotent stem cells. Cell Mol Life Sci 2018; 75: 1191-1203.

[3] Weinberger L, Ayyash M, Novershtern N and Hanna JH. Dynamic stem cell states: naive to primed pluripotency in rodents and humans. Nat Rev Mol Cell Biol 2016; 17: 155-169.

[4] Hayashi Y, Furue MK, Okamoto T, Ohnuma K, Myoishi Y, Fukuhara Y, Abe T, Sato JD, Hata R and Asashima M. Integrins regulate mouse embryonic stem cell self-renewal. Stem Cells 2007; 25: 3005-3015.

[5] Nichols J and Smith A. Naive and primed pluripotent states. Cell Stem Cell 2009; 4: 487-492.

[6] Surani MA, Hayashi K and Hajkova P. Genetic and epigenetic regulators of pluripotency. Cell 2007; 128: 747-762.

[7] Deb A, Sarkar A and Ghosh Z. Dissecting the variation in transcriptional circuits between naive and primed pluripotent states. FEBS Lett 2017; 591: 2362-2375.

[8] Sato N, Meijer L, Skaltsounis L, Greengard P and Brivanlou AH. Maintenance of pluripotency in human and mouse embryonic stem cells through activation of Wnt signaling by a pharmacological GSK-3-specific inhibitor. Nat Med 2004; 10: 55-63.

[9] Tee WW and Reinberg D. Chromatin features and the epigenetic regulation of pluripotency states in ESCs. Development 2014; 141: 2376-2390.

[10] Zhang X, Li B, Li W, Ma L, Zheng D, Li L, Yang W, Chu M, Chen W, Mailman RB, Zhu J, Fan G, Archer TK and Wang Y. Transcriptional repression by the BRG1-SWI/SNF complex affects the pluripotency of human embryonic stem cells. Stem Cell Reports 2014; 3: 460-474.

[11] Kunath T, Saba-El-Leil MK, Almousailleakh M, Wray J, Meloche S and Smith A. FGF stimula-

tion of the Erk1/2 signalling cascade triggers transition of pluripotent embryonic stem cells from self-renewal to lineage commitment. Development 2007; 134: 2895-2902.
[12] Hall J, Guo G, Wray J, Eyres I, Nichols J, Grotewold L, Morfopoulou S, Humphreys P, Mansfield W, Walker R, Tomlinson S and Smith A. Oct4 and LIF/Stat3 additively induce Kruppel factors to sustain embryonic stem cell self-renewal. Cell Stem Cell 2009; 5: 597-609.
[13] Niwa H, Ogawa K, Shimosato D and Adachi K. A parallel circuit of LIF signalling pathways maintains pluripotency of mouse ES cells. Nature 2009; 460: 118-122.
[14] Xie X, Fu Y and Liu J. Chemical reprogramming and transdifferentiation. Curr Opin Genet Dev 2017; 46: 104-113.
[15] Chen G, Guo Ye, Li C, Li S and Wan X. Small molecules that promote self-renewal of stem cells and somatic cell reprogramming. Stem Cell Rev Rep 2020; 16: 511-523.
[16] Boulton TG, Stahl N and Yancopoulos GD. Ciliary neurotrophic factor/leukemia inhibitory factor/interleukin 6/oncostatin M family of cytokines induces tyrosine phosphorylation of a common set of proteins overlapping those induced by other cytokines and growth factors. J Biol Chem 1994; 269: 11648-11655.
[17] Cartwright P, McLean C, Sheppard A, Rivett D, Jones K and Dalton S. LIF/STAT3 controls ES cell self-renewal and pluripotency by a Myc-dependent mechanism. Development 2005; 132: 885-896.
[18] Moratilla A, Maza DS, Martin MC and Miguel MD. Inhibition of PKCε induces primordial germ cell reprogramming into pluripotency by HIF1&2 upregulation and histone acetylation. Am J Stem Cells 2021; 10: 1-17.
[19] Silva J and Smith A. Capturing pluripotency. Cell 2008; 132: 532-536.
[20] Dutta D, Ray S, Home P, Larson M, Wolfe MW and Paul S. Self-renewal versus lineage commitment of embryonic stem cells: protein kinase C signaling shifts the balance. Stem Cells 2011; 29: 618-628.
[21] Nichols J and Smith A. Pluripotency in the embryo and in culture. Cold Spring Harb Perspect Biol 2012; 4: a008128.
[22] Ying QL, Nichols J, Chambers I and Smith A. BMP induction of Id proteins suppresses differentiation and sustains embryonic stem cell self-renewal in collaboration with STAT3. Cell 2003; 115: 281-292.
[23] Rajendran G, Dutta D, Hong J, Paul A, Saha B, Mahato B, Ray S, Home P, Ganguly A, Weiss ML and Paul S. Inhibition of protein kinase C signaling maintains rat embryonic stem cell pluripotency. J Biol Chem 2013; 288: 24351-24362.
[24] Dai YJ, Li JS, Li MY, Liu ZH, Liu J, An LY and Du FL. Methyl-CpG-binding domain 3 (Mbd3) is an important regulator for apoptosis in mouse embryonic stem cells. Am J Transl Res 2020; 12: 8147-8161.
[25] Takashima Y, Guo G, Loos R, Nichols J, Ficz G, Krueger F, Oxley D, Santos F, Clarke J, Mansfield W, Reik W, Bertone P and Smith A. Resetting transcription factor control circuitry toward ground-state pluripotency in human. Cell 2014; 158: 1254-1269.
[26] Liu J, Zhu XM, Li J, Liu ZH, Liu YH, Xue F, Yang L, An LY , Chen CH, Presicce GA, Zheng QP and Du FL. Deriving rabbit embryonic stem cells by small molecule inhibitors. Am J Transl Res 2019; 11: 5122-5133.
[27] Macfarlan TS, Gifford WD, Driscoll S, Lettieri K, Rowe HM, Bonanomi D, Firth A, Singer O, Trono D and Pfaff SL. Embryonic stem cell potency fluctuates with endogenous retrovirus activity. Nature 2012; 487: 57-63.
[28] Takahashi K and Yamanaka S. Induction of pluripotent stem cells from mouse embryonic and adult fibroblast cultures by defined factors. Cell 2006; 126: 663-676.
[29] Kouzarides T. Chromatin modifications and their function. Cell 2007; 128: 693-705.
[30] Shahbazian MD and Grunstein M. Functions of site-specific histone acetylation and deacetylation. Annu Rev Biochem 2007; 76: 75-100.
[31] Wang F, Kou Z, Zhang Y and Gao S. Dynamic reprogramming of histone acetylation and methylation in the first cell cycle of cloned mouse embryos. Biol Reprod 2007; 77: 1007-1016.
[32] Zhang Y, Xiang Y, Yin Q, Du Z, Peng X, Wang Q, Fidalgo M, Xia W, Li Y, Zhao ZA, Zhang W, Ma J, Xu F, Wang J, Li L and Xie W. Dynamic epigenomic landscapes during early lineage specification in mouse embryos. Nat Genet 2018; 50: 96-105.
[33] Chen M, Zhu Q, Li C, Kou X, Zhao Y, Li Y, Xu R, Yang L, Yang L, Gu L, Wang H, Liu X, Jiang C and Gao S. Chromatin architecture reorganization in murine somatic cell nuclear transfer embryos. Nat Commun 2020; 11: 1813.
[34] Brochard V and Beaujean N. Somatic reprograming by nuclear transfer. Methods Mol Biol 2021; 2214: 109-123.
[35] Hormanseder E, Simeone A, Allen GE, Bradshaw CR, Figlmuller M, Gurdon J and Jullien J. H3K4 methylation-dependent memory of somatic cell identity inhibits reprogramming and development of nuclear transfer embryos. Cell Stem Cell 2017; 21: 135-143.
[36] Xie B, Zhang H, Wei R, Li Q, Weng X, Kong Q and Liu Z. Histone H3 lysine 27 trimethylation acts as an epigenetic barrier in porcine nucle-

ar reprogramming. Reproduction 2016; 151: 9-16.
[37] Bibikova M, Laurent LC, Ren B, Loring JF and Fan JB. Unraveling epigenetic regulation in embryonic stem cells. Cell Stem Cell 2008; 2: 123-134.
[38] Armstrong L. Epigenetic control of embryonic stem cell differentiation. Stem Cell Rev Rep 2012; 8: 67-77.
[39] Chen J, Liu H, Liu J, Qi J, Wei B, Yang J, Liang H, Chen Y, Chen J, Wu Y, Guo L, Zhu J, Zhao X, Peng T, Zhang Y, Chen S, Li X, Li D, Wang T and Pei D. H3K9 methylation is a barrier during somatic cell reprogramming into iPSCs. Nat Genet 2013; 45: 34-42.
[40] Wang Y, Bi Y and Gao S. Epigenetic regulation of somatic cell reprogramming. Curr Opin Genet Dev 2017; 46: 156-163.
[41] Niu L, Shen W, Shi Z, Tan Y, He N, Wan J, Sun J, Zhang Y, Huang Y, Wang W, Fang C, Li J, Zheng P, Cheung E, Chen Y, Li L and Hou C. Three-dimensional folding dynamics of the Xenopus tropicalis genome. Nat Genet 2021; 53: 1075-1087.
[42] Song J, Saha S, Gokulrangan G, Tesar PJ and Ewing RM. DNA and chromatin modification networks distinguish stem cell pluripotent ground states. Mol Cell Proteomics 2012; 11: 1036-1047.
[43] Matoba S, Liu Y, Lu F, Iwabuchi KA, Shen L, Inoue A and Zhang Y. Embryonic development following somatic cell nuclear transfer impeded by persisting histone methylation. Cell 2014; 159: 884-895.
[44] Shinagawa T, Takagi T, Tsukamoto D, Tomaru C, Huynh LM, Sivaraman P, Kumarevel T, Inoue K, Nakato R, Katou Y, Sado T, Takahashi S, Ogura A, Shirahige K and Ishii S. Histone variants enriched in oocytes enhance reprogramming to induced pluripotent stem cells. Cell Stem Cell 2014; 14: 217-227.
[45] Chung YG, Matoba S, Liu Y, Eum JH, Lu F, Jiang W, Lee JE, Sepilian V, Cha KY, Lee DR and Zhang Y. Histone demethylase expression enhances human somatic cell nuclear transfer efficiency and promotes derivation of pluripotent stem cells. Cell Stem Cell 2015; 17: 758-766.
[46] Wang L, Miao YL, Zheng X, Lackford B, Zhou B, Han L, Yao C, Ward JM, Burkholder A, Lipchina I, Fargo DC, Hochedlinger K, Shi Y, Williams CJ and Hu G. The THO complex regulates pluripotency gene mRNA export and controls embryonic stem cell self-renewal and somatic cell reprogramming. Cell Stem Cell 2013; 13: 676-690.
[47] Zhang T, Wei G, Millard CJ, Fischer R, Konietzny R, Kessler BM, Schwabe JWR and Brockdorff N. A variant NuRD complex containing PWWP2A/B excludes MBD2/3 to regulate transcription at active genes. Nat Commun 2018; 9: 3798.
[48] Torchy MP, Hamiche A and Klaholz BP. Structure and function insights into the NuRD chromatin remodeling complex. Cell Mol Life Sci 2015; 72: 2491-2507.
[49] Allen HF, Wade PA and Kutateladze TG. The NuRD architecture. Cell Mol Life Sci 2013; 70: 3513-3524.

Table S1. Gene list for **Figure 1F**

	Wnt signaling pathway		PI3K-Akt signaling pathway		MAPK signaling pathway		Focal adhesion		Chemokine signaling pathway		ECM-receptor interaction
Gene List	*Notum*	*Sfrp1*	*Ccne2*	*Col9a2*	*Map3k6*	*Fgf23*	*Capn2*	*Ccnd2*	*Adcy7*	*Ccl9*	*Col6a1*
	Vangl1	*Fzd9*	*Il6ra*	*Ppp2r2c*	*Fgfr3*	*Pdgfa*	*Shc4*	*Thbs2*	*Cxcl16*	*Ccl11*	*Sv2a*
	Wnt3a	*Peg12*	*Csf3r*	*Vegfc*	*Il1rap*	*Efna1*	*Jun*	*Itga9*	*Cxcl3*	*Arr3*	*Thbs3*
	Dkk1		*Creb3l2*	*Col4a1*	*Fgf10*	*Flt1*	*Col6a4*	*Col6a1*	*Pf4*	*Gngt2*	*Col6a2*
	Rac2		*Itgb3*	*Chad*	*Gadd45b*	*Map3k5*	*Shc2*	*Flna*	*Cxcl2*	*Hck*	*Itga9*
	Sfrp5		*Eif4e1b*	*Egfr*	*Map2k6*	*Cacna1h*	*Parva*	*Igf1*	*Gnb4*	*Bcar1*	*Col6a5*
	Ccnd3		*Pdgfa*	*Sgk1*	*Relb*	*Pdgfrb*	*Thbs3*	*Cav1*	*Shc4*	*Cxcl12*	*Tnxb*
	Prickle3		*Fgfr3*	*Fgf23*	*Rasgrp1*		*Fyn*	*Flnc*	*Dock2*	*Rasgrp2*	*Thbs2*
	Gpc4		*Fgf3*	*Lpar1*	*Hspa2*		*Mapk10*	*Prkcb*	*Plcb2*	*Gng3*	*Reln*
	Sox17		*Lpar5*	*Col4a2*	*Fgf3*		*Bcar1*		*Prkcb*	*Ccl6*	*Col6a4*
	Wif1		*Fgf10*	*Efna1*	*Kit*		*Col6a5*		*Shc2*	*Cxcl1*	*Fras1*
	Fzd10		*Lamc2*	*Flt1*	*Map3k8*		*Tnxb*		*Cxcl10*	*Cxcl5*	*Lamb3*
	Fzd5		*Osm*	*Jak3*	*Mras*		*Reln*		*Ccl7*	*Arrb1*	*Frem1*
	493044		*Col6a3*	*Lama1*	*Kdr*		*Lamb3*		*Gng2*	*Ccl2*	*Frem2*
	4G20Rik		*Ccnd3*	*Col1a1*	*Rac2*		*Col6a2*		*Ccl28*		
	Frat1		*Kdr*	*Pdgfrb*	*Vegfc*		*Parvg*		*Gng4*		
	Prickle2		*Kit*		*Egfr*		*Myl9*		*Ccl3*		

Table S2. Sequences of primers used for qPCR

Gene Symbol	Forward Primer (5'-3')	Reverse Primer (5'-3')	PCR Condition
kdm4a	AACTTCAGCCGCTACATTGC	ATCAATATCGTCGTAGGATGTTCG	95°C 15 s, Annealing/Extension 60°C 60 s, 40 Cycles
kdm4b	ACAGTACAACATCCAGAAGAAGG	CGCTCCAAGTCATCGAAGTC	95°C 15 s, Annealing/Extension 60°C 60 s, 40 Cycles
kdm4c	GGAGGACATGGATCTCTACAGTAT	GGCTAGTCTTTCAAGTCGCTTT	95°C 15 s, Annealing/Extension 60°C 60 s, 40 Cycles
kdm4d	GCTCCTGCTCCTCAGTAGAC	GCAGAATCTCTTCAGGGATGTG	95°C 15 s, Annealing/Extension 60°C 60 s, 40 Cycles
kdm5a	CAATCTGGTGTCAGCCTTATGG	CGTCTTGTTCTCTTTGGTGGAA	95°C 15 s, Annealing/Extension 60°C 60 s, 40 Cycles
kdm5b	TGATGACAGTTACCACACCTTCT	AGTCCCTTGCTGCTTGTTCA	95°C 15 s, Annealing/Extension 60°C 60 s, 40 Cycles
kdm5c	AGAAGGCAAGGAGGAACTGAG	CGGGAACACATTCGGCATAC	95°C 15 s, Annealing/Extension 60°C 60 s, 40 Cycles
kdm5d	TTCAGTCTGGAGCTAATCTTGTG	TTCCTCGTCTACTGTAGCAACT	95°C 15 s, Annealing/Extension 60°C 60 s, 40 Cycles
kdm6a	CGCTTTCGGTGATGAGGAA	GAAACCTCACGAACCCGAA	95°C 15 s, Annealing/Extension 60°C 60 s, 40 Cycles
kdm6b	CGGTCCTGCTACAGTTCTGT	GACCTCCACCGTATGTTCAC	95°C 15 s, Annealing/Extension 60°C 60 s, 40 Cycles
lin28a	CCCTGGTGGTGTGTTCTGTA	CATTCCTTGGCATGATGGTCTA	95°C 15 s, Annealing/Extension 60°C 60 s, 40 Cycles
myc	GAGCCCACCACACACATTCT	GGGGAACAGATTCTGGCAGT	95°C 15 s, Annealing/Extension 60°C 60 s, 40 Cycles
pou5f1	GAGGAAGCCGACAACAATGAG	TGTGAGTGATCTGCTGTAGGGAG	95°C 15 s, Annealing/Extension 60°C 60 s, 40 Cycles
sox2	GGTTACCTCTTCCTCCCACTCCAGG	TGTGCCGTTAATGGCCGTGCC	95°C 15 s, Annealing/Extension 60°C 60 s, 40 Cycles
gdpd5	CTTCTCCTGCCACAGTCTCC	GTGCTCCGTGTGTTTCTTCC	95°C 15 s, Annealing/Extension 60°C 60 s, 40 Cycles
h19	ACGGAGCAGTGATCGGTGT	AGCAGCAGAGAAGTGTTAGCT	95°C 15 s, Annealing/Extension 60°C 60 s, 40 Cycles
pfkfb4	GAGCCAGATGAAGAGGACGAT	CAAACTCCAGCGGGTAGTGA	95°C 15 s, Annealing/Extension 60°C 60 s, 40 Cycles
thoc5	CTGAAGGAGATTGAGGTGAAGAG	GTGCCTGGCAGTCTCATACT	95°C 15 s, Annealing/Extension 60°C 60 s, 40 Cycles
GAPDH	GTGGCAAAGTGGAGATTGTTG	CTCCTGGAAGATGGTGATGG	95°C 15 s, Annealing/Extension 60°C 60 s, 40 Cycles

Table S3. Sequences of siRNA and siRNA-nc used for knockdown

Gene Symbol	RNA oligo sequences 21nt guide (5'→3')	RNA oligo sequences 21nt passenger (5'→3')
kdm6a-siRNA	UUAAACUAGACUCAUAGUCUG	GACUAUGAGUCUAGUUUAAAG
	AUUCGUAGGAGACACAAACUU	GUUUGUGUCUCCUACGAAUCC
	UUAAAUAGCAUUUAAUAGCAU	GCUAUUAAAUGCUAUUUAAAU
kdm4d-siRNA	UUCUUCAUAUCCACUUAAGUG	CUUAAGUGGAUAUGAAGAAGG
	AAUAAAUAAAGAAGACUUGCU	CAAGUCUUCUUUAUUUAUUUU
	GGACUAGAGUUGUCACUUAAG	UAAGUGACAACUCUAGUCCCU
kdm6a-siRNA-nc	CGAUCGUUGUCAGAAGUAAGU	UUACUUCUGACAACGAUCGGA
kdm4d-siRNA-nc	CGGCGUCAAUACGGGAUAAUA	UUAUCCCGUAUUGACGCCGGG

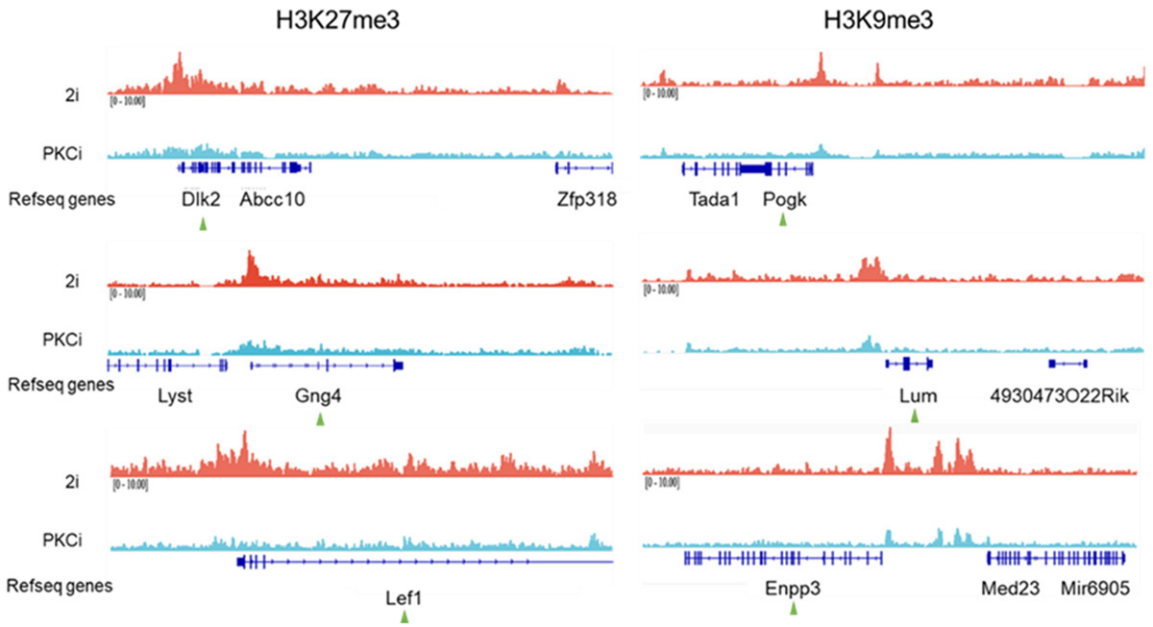

Figure S1. A genome browser view of three examples of DEG on H3K27me3 and H3K9me3 between the two types of mESC. The H3K27me3 modification signal of stem cell-specific genes (green triangle markers gene) in PKCi-mESC were greatly reduced in the proximal TSS segment. In addition, H3K9me3 in the TTS segment were significantly reduced. PKCi: PKCi-mESC, 2i: 2i-mESC.